Asymmetric Magnetization Switching in Perpendicular Magnetic Tunnel Junctions: Role of the Synthetic Antiferromagnet's Fringe Field

M. Lavanant, P. Vallobra, S. Petit Watelot, V. Lomakin, A.D. Kent, J. Sun, and S. Mangin

Phys. Rev. Applied **11**, 034058 — Published 25 March 2019

DOI: 10.1103/PhysRevApplied.11.034058

Asymmetric magnetization switching in perpendicular magnetic tunnel junctions: Role of the synthetic antiferromagnet's fringe field

M. Lavanant[1], P. Vallobra[1], S. Petit Watelot[1], V. Lomakin[2] A. D. Kent[3] J. Sun[4] and S. Mangin*[1]

* stephane.mangin@univ-lorraine.fr

1 Institut Jean Lamour, CNRS-UMR 7198, Université de Lorraine, 2, allée Guinier, F-5400 Nancy, France
2 Center for Memory and Recording Research, University of California San Diego, 9500 Gilman Dr. La Jolla, CA 92093-0401 USA
3 Center for Quantum Phenomena, Department of Physics, New York University, 726 Broadway, New York, NY 10003 USA
4 IBM T.J. Watson Research Center, IBM, 1101 Kitchawan Rd, Rt 13 Yorktown Heights, NY, 10598, USA

The field and current induced magnetization reversal of a Co-Fe-B layer in a perpendicular magnetic tunnel junction (pMTJs) has been studied at room temperature. The magnetization switching probability from the parallel (P) state to the anti-parallel (AP) state and from AP to P is found to be asymmetric. We observe that this asymmetry depends on the magnetic configuration of the synthetic antiferromagnetic (SAF). The state diagram and the energy landscape are compared for two SAF configurations. We conclude that the asymmetry is due to the inhomogeneity of the fringe field generated by the SAF. Our study highlights the role of reference-layer fringe field on the free-layer's energy barrier height which has to be carefully control for memory application.

Introduction

Current induced manipulation of magnetization has been a subject of great interest since the prediction of spin transfer torque (STT) by Berger [1] and Slonczewski [2] in 1996. It has led to a new magnetic memory technology namely spin-transfer torque magnetic random access memories (STT-MRAM). Such devices are composed of magnetic tunnel junctions with electrodes exhibiting a strong perpendicular magnetic anisotropy (pMTJs) [3-6]. In these devices the switching current is directly proportional to the energy barrier for thermally activated magnetization reversal [6,7]. Indeed, devices composed of materials with large perpendicular magnetic anisotropy (PMA) have been shown to combine both a good thermal stability and exhibit efficient current induced switching [6-8]. To further improve STT-MRAM device the switching energy and the switching time still need to be reduced [10], both of which depend on the energy barrier. The study and the characterization of the energy barrier is therefore crucial for improving the performance of STT-MRAM.

Magnetic tunnel junctions are made of a thin insulating layer sandwiched between a free magnetic layer that can be switched and a reference layer. The latter acts as a spin polarizer for the current and gives rise to a dipolar field with a strong out of plane component. This magnetic field, also called a fringe field, may create an asymmetry in the magnetization reversal of the free layer [11]. In order to reduce this effect, "synthetic antiferromagnetic" structures (SAF) have been used to reduce the fringe field. The SAF is composed of two magnetic layers antiferromagnetically coupled through a non-magnetic layer [12-14]. These layers magnetization are antiparallel and thus have a net magnetization close to zero and, to a first approximation, the average fringe field emitted by the SAF is also close to zero. However, the free layer still experiences a dipolar field associated with the SAF, as one layer of the SAF is closer to the free layer than the other. Moreover, the shape and the size of the device also influence the fringe field value and homogeneity [15,16].

In this paper the role of the fringe field from the SAF on the free layer switching is studied. First the probability of non switching for the free layer as a function of the voltage and magnetic field switching is obtained. The latter provides information on the energy barrier to thermally activated magnetization switching. The respective effect of a compensated SAF (antiparallel magnetized layers) and a saturated SAF (parallel magnetized layers of the SAF) on the switching probability and the switching state diagram is investigated.

Experiments

A $[Co(0.25nm)/Pt(0.8nm)]_{14}$/Ru (0.9nm)/Co (0.3mn)/$[Co(0.25nm)/Pd(0.8nm)]_4$/ Co(0.25nm)/Pt(0.8nm) / Co(0.25nm)/Ta(0.3nm)/ Co-Fe-B(1.3nm)/ MgO(0.9nm)/ Co-Fe-B(0.8nm)/Capping sample has been grown by DC magnetron sputtering. The Co-Fe-B (0.8nm) is the free layer and the Co (0.3mn)/$[Co(0.25nm)/Pd(0.8nm)]_4$/ Co(0.25nm)/Pt(0.8nm)/ Co(0.25nm)/Ta(0.3nm)/ Co-Fe-B(1.3nm) is the reference layer. The layers are separated by an MgO tunnel barrier. The reference layer is antiferromagnetically coupled through the Ru (0.9nm) to the $[Co(0.25)/Pt(0.8nm)]_{14}$ pinning layer. The reference layer and the pinning layer together form a Synthetic AntiFerromagnetic (SAF layer). We are interested in the switching behavior of the free layer magnetization between its two stable states, parallel (P) and antiparallel (AP) to the reference layer. The SAF was made to have an antiparallel alignment of the reference and the pinning layer in order to decrease the fringe field. However, in this study, to test the influence of the fringe field, we also consider the case where they are parallel. We call these configurations respectively “compensated” (antiparallel) and “saturated” (parallel). Let us first consider the case when the SAF is compensated. All measurements presented in this paper were performed at room temperature.

Figure 1a) shows the resistance of the pMTJ as a function of the voltage for the AP to P transition (orange) and the P to AP (blue) for numerous sweeps. There is a distribution of switching voltages. From these data the probability of non-switching as a function of the voltage a shown in figure 1b) could be determined [16]. Our aim is to deduce the energy barrier associated with each transition from the corresponding probability of non-switching as it has been discussed in [18].

In order to do so, a single energy barrier $\Delta E(H)$ representing the thermal stability of a tunnel junction is considered between the two stable states [19]. Starting from the LLG equation describing the motion of the magnetization, [20,21], it is possible to include the thermal fluctuation contribution based on the pioneering works Néel [22] and Brown [23]. It has been shown that the effect of the voltage can be considered as an effective temperature [24,25]. Following the same idea the non-conservative term of the STT is considered as an effective temperature in the LLG equation. Koch found then that the experimental values of STT driven transitions probability in spin valves were in good agreement with this theory [26]. The switching probability in MTJs can then be theoretically found using the same models. Values of the parameters needed to characterize the STT switching in MTJs can be found in the literature. Ab-initio calculations have shown that in MTJ the STT non-conservative torque depends linearly on the applied voltage in pMTJs [27] and this has also been measured and verified experimentally [28,29].

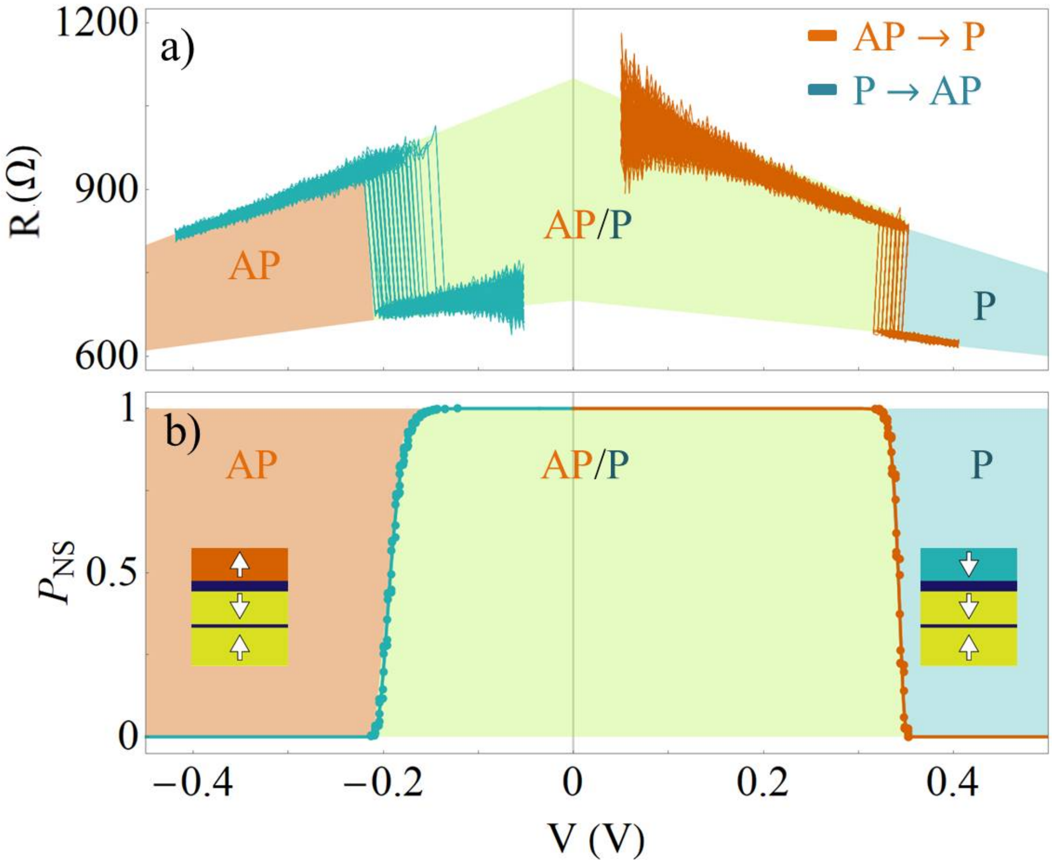

Figure 1 : Switching distribution for a $70 \times 100nm^2$ pMTJ with a compensated SAF for an applied field $\mu_0 H = -30mT$ a) Resistance as a function of the applied voltage for voltage close to the AP to P transition (orange) and close to the P to AP (blue) for 1000 voltages sweeps b) non-switching probabilities deduced from a).

This leads us to the expression of the non-switching probability P_{NS} in a MTJ that follows for a voltage V sweeping with a rate r (10V/s) experiment at fixed field H_{app} :

$$P_{NS}(V, H_{app}) = \exp\left[-\frac{1}{\tau_0 r}\int_0^V \exp\left(-\frac{\Delta E_0}{k_B T}(1-\frac{H_{app}- H_{off}}{H_{sw0}})^\eta\left(1-\frac{v}{V_{sw0}}\right)dv\right)\right]$$

Where $\frac{1}{\tau_0}$ is the attempt frequency of the switching (we have chosen 1 GHz), ΔE_0 the energy barrier of the transition, η is a parameter depending on the geometry and the switching type, here taken at $\eta = \frac{3}{2}$ [19]. H_{sw0} and V_{sw0} are respectively the zero-temperature switching field and the switching voltage and H_{off} is in the first approximation the mean value of the average perpendicular fringe field. This equation is set under three main hypotheses: the measurement is quasi-static, the conservative part of the STT is neglected, and the Slonczewski spin-torque is considered as an effective temperature.

The voltage sweepings presented in figure 1 are repeated for different fixed fields, and using the expression of the probability of non-switching, we obtain the dependence of the energy barrier of each transition as a function of the applied field $\Delta E(H_{app}) = \frac{\Delta E_0}{k_B T}(1-\frac{H_{app}- H_{off}}{H_{sw0}})^\eta$. Figure 2a) shows the energy barrier dependence as a function of the applied field for the two SAF configurations, compensated on the left (low fringe field) and saturated on the right (large fringe field). Figure 2b) displays the corresponding state diagrams obtained by recording the switching voltage as a function of the applied field for both transitions and both configurations as described in Ref [30-32]. Insets are schematics of the stack magnetic configurations. The results presented in figure 2 were obtained for a 70×100nm² junction, but similar results were obtained for various junction sizes, from 60×80nm² to 100×240nm² (not shown).

For both configurations of the SAF, the state diagram presents an offset field that we link in a first approximation to the average perpendicular component of the fringe field. We define $\mu_0 H_{off}$ as the central value of the field hysteresis loop for no voltage. We obtain $\mu_0 H_{off} = -30mT$ in the compensated configuration and $\mu_0 H_{off} = 120mT$in the saturated one. Their positions are noted in figure 2 as the vertical black lines. The evolution of the energy barrier as a function of field can be fitted by the above expression, as shown in figure 2a). We observe that the energy barriers for P to AP and AP to P transitions versus applied field vary in opposite senses---they have opposite signs of their slopes---for both SAF configurations. They also cross at a certain field. At this field the energy barriers to switch from P to AP and from AP to P are equal. We expected that the latter field would correspond to the applied field that compensates the average fringe field, which is clearly not the case.

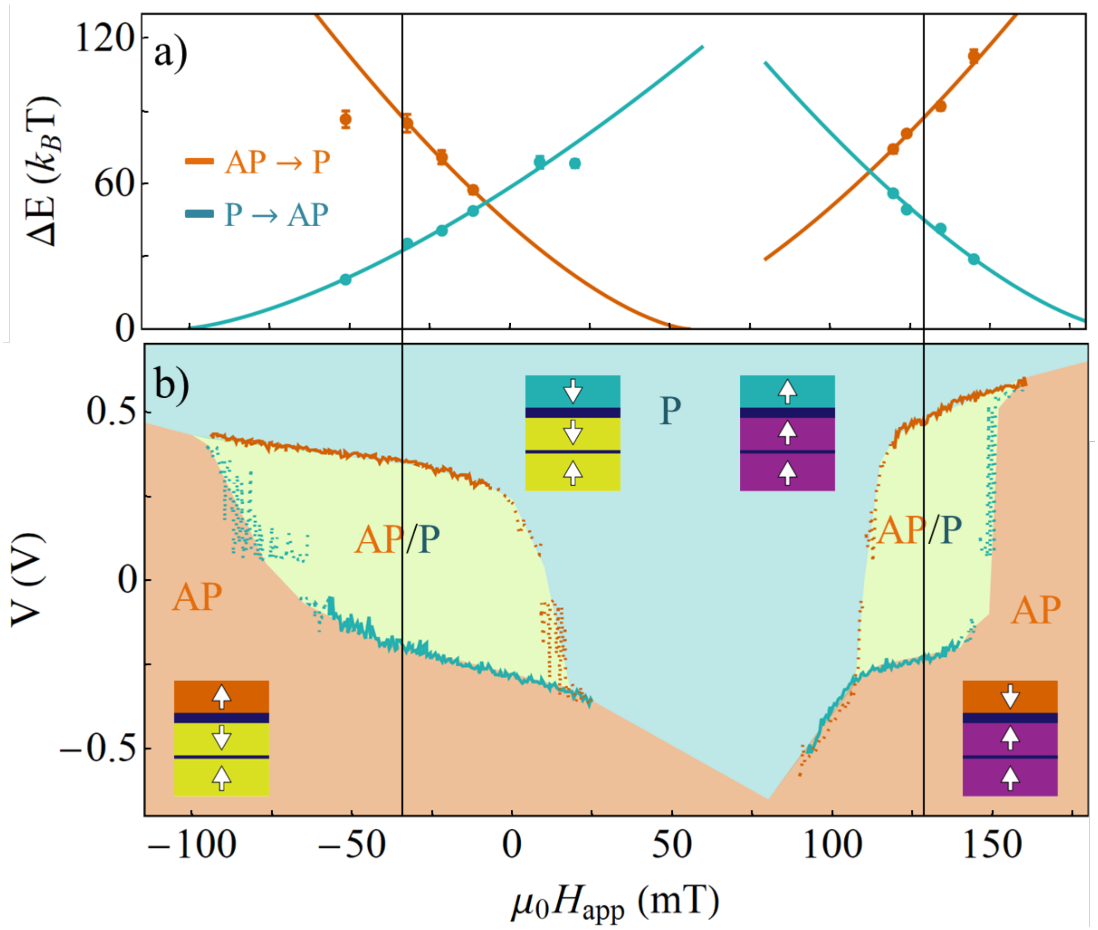

Figure 2: a) Evolution of the energy barrier for the AP to P transition (orange) and P to AP (blue) transitions as a function of the applied field with a compensated or a saturated SAF. b) Evolution of the switching voltage for the AP to P transition (orange) and P to AP (blue) transitions as a function of the applied field with a compensated or a saturated SAF. The inset shows sketches of the P and AP states for the two SAF magnetic configurations (compensated and saturated).

Both state diagrams presented in figure 2b) are centered around the net offset field value$\mu_0 H_{off}$. However there is an asymmetry of the switching voltages between the two transitions. The switching voltage from AP to P is larger than from P to AP. This effect is clearly seen in figure 1 as the measurement was done close to H_{off}. We clearly observe that the non-switching probabilities also have different dependencies on the voltage.

A strong effect of the SAF magnetic state is observed in both the voltage and field driven switching. In the saturated SAF state the state diagram width is reduced by two thirds and the switching voltages are shifted toward larger positive values for the AP to P transition. These observations indicate that the asymmetry in switching voltages and energy barriers cannot be described with a simple macrospin model, thus we use micromagnetic simulation to describe our experiments.

Modeling

The software Fastmag developed at UCSD [33] was used to study the switching process of the free layer at a given applied voltage, a given applied field and zero temperature. This software uses a finite element method to solve the LLG equation. We computed a $60\times80nm^2$ MTJ. We also considered a zero field-like torque and a coefficient of the Slonczewki term $a_V=6.37\times10^3$ $A.m^{-1}.V^{-1}$[34]. The thickness resolution is 1 nm. We also considered the [Co|Pd] and [Co|Pt] multilayers to be one single block. The free layer (1), the barrier layer (gap) and 1.3nm Co-Fe-B layer (2) are set to be 1nm thick each, the Co (0.3mn)/$[Co(0.25nm)/Pd(0.8nm)]_4$/ Co(0.25nm)/Pt(0.8nm) /Co(0.25nm) layer (layer 3) to be 5nm thick and the $[Co(0.25nm)/Pt(0.8nm)]_{14}$ layer (layer 4) to be 15nm thick. The surface exchange coupling between the upper SAF layer and the reference layer is set to $1.242\times10^{-3}J.m^{-2}$, and the one between the two layers of the SAF is set to $-1.242\times10^5J.m^{-2}$. The rest of the stack parameters is shown on table 1[34,35] :

Layers	$K(J.m^{-3})$	$M_S(A.m^{-1})$	$A_x(J.m^{-1})$	α (–)
1 & 2	$7.2\cdot10^5$	$10.5\cdot10^5$	$1.3\cdot10^{-11}$	0.01
3 & 4	$3\cdot10^5$	$3.5\cdot10^5$	$1.3\cdot10^{-11}$	0.01

Table 1: Stack parameters used for the Fastmag simulations, the anisotropy constant K, the saturated magnetization M_S, the exchange coupling and the damping.

As already demonstrated in order to reproduce the experimental state diagram using an analytical or numerical modeling the uniaxial symmetry needs to be broken. In the present computation we have introduced a tilt of 0.6 degree in the magnetocrystalline anisotropy axis that is sufficient to break the uniaxial symmetry [32].We have been able to follow the magnetic configurations during the STT driven magnetization switching, as seen in figure 3 c,d,e,f. This allows us to compare the nucleation points of the reversal depending on the transition. In the case of the compensated SAF, the nucleation point depends on the transition: it occurs at an edge for the P to AP transition (figure 3-c) and at the center of the layer for the AP to P transition (figure 3-d). In the case of the saturated SAF, the nucleation for both transitions occurs at the edge of the sample (figure 3-e,f).

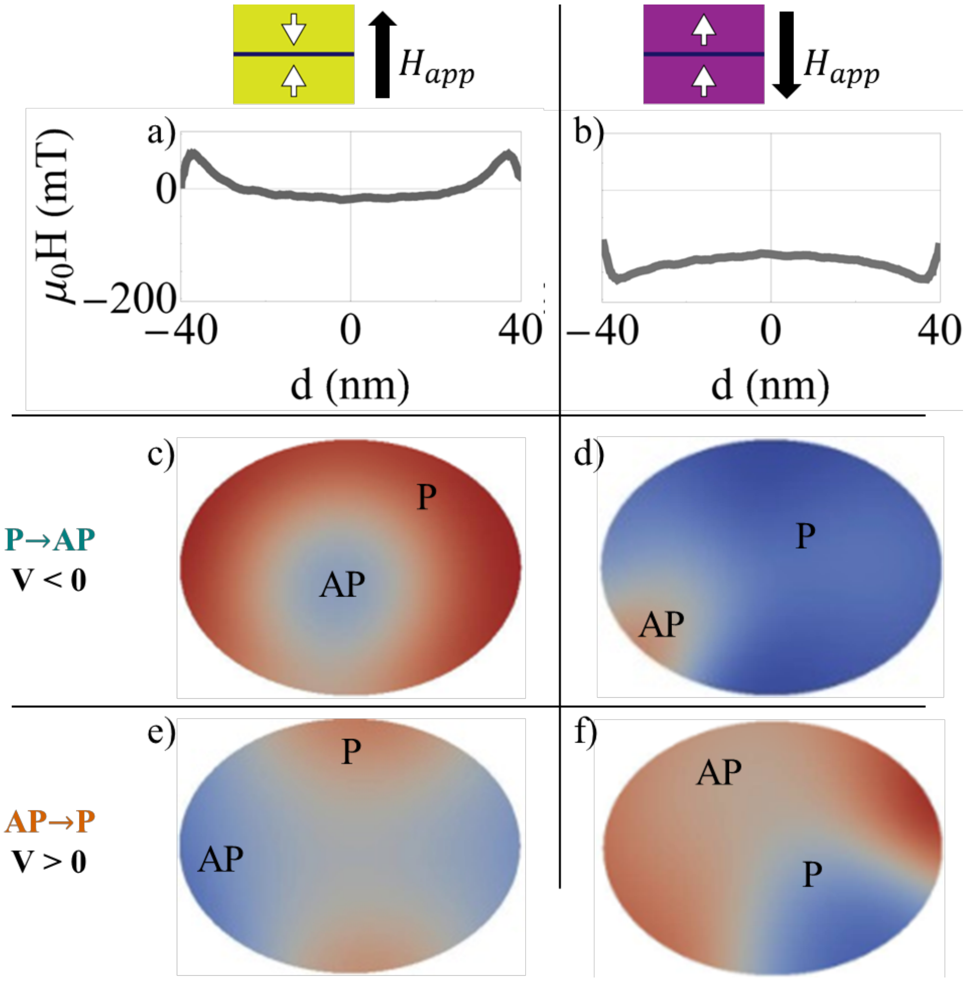

Figure 3 : I) Micromagnetic simulations of the reference layers fringe field of a 60×80nm[2] element obtained from Fastmag simulations at the free layer position for a) the compensated SAF (blue) and b) saturated SAF (orange) configurations, II) Micromagnetic configuration of the nucleation process for the P to AP (first line) and AP to P (second line) STT-driven switching in the a) compensated SAF (AP blue, P red) and b) "no SAF" (AP red, P blue) configurations.

The strength of the dipolar field as a function of the distance from the center of the sample is also plotted in Fig.3-a, b for both SAF states and both transitions. We observe that the strength of the fringe field depends on the configuration of the SAF as intuited before. Also in both SAF configurations the stray field is inhomogeneous along the width of the junction. Even in the compensated case (figure 3 a), it is close to zero at the center of the junction and higher at its edges. Since we showed in figure 3 that the fringe field has a strong influence on the phase diagram we claim that the peak in the fringe field at the edges of the sample can explain the asymmetry in the energy barrier of the transitions.

Conclusion

The influence of the fringe field from the synthetic antiferromagnet on the switching behavior has been shown experimentally by measuring the switching probability the P to AP and AP to P transitions. The observed asymmetry between the two transitions cannot be explained by the presence of a homogeneous fringe field from the SAF. We demonstrated thanks to micromagnetic simulations that this asymmetry observed in quasi-static measurements is likely associated with inhomogeneities of the fringe field of the SAF at the edge of the sample. Similar asymmetry has been reported in the "nano-second" dynamic switching regime for perpendicular MTJ [36]. Those inhomogeneities favor domain nucleation in certain area of the free layer depending on the transition.

Acknowledgements

Research at NYU was supported by Grant No. NSF- DMR-1610416. Research in Nancy was supported by the ANR-NSF COMAG project, ANR-13-IS04-0008-01, by the ANR-Labcom LSTNM project ANR-13-LAB2-0008, by the French PIA project 'Lorraine Université d'Excellence', reference ANR-15-IDEX-04-LUE. Experiments were performed using equipment from the TUBE Davm funded by FEDER (EU), ANR -14-IDEX-0001, Région Grand Est and Metropole Grand Nancy.

References

[1] L. Berger, "Emission of spin waves by a magnetic multilayer traversed by a current", Phys. Rev. B, **54**,13 (1996)

[2] J.C. Slonczewski, "Current-driven excitation of magnetic multilayers", J. Magn. Magn. Mater.,**159**(1-2):L1–L7 (1996)

[3] D.C. Worledge, G. Hu, P.L.Trouilloud,D.W. Abraham, S. Brown,M.C. Gaidis, J. Nowak, E.J. O'Sullivan, R.P. Robertazzi, J.Z. Sun, W.J. Gallagher, "Switching distributions and write reliability of perpendicular spin torque,", MRAM IEDM (2010)

[4] S. Ikeda, K. Miura, H. Yamamoto, K. Mizunuma, H. D. Gan, M. Endo, S. Kanai, J. Hayakawa, F. Matsukura and H. Ohno, "A perpendicular-anisotropy CoFeB–MgO magnetic tunnel junction," Nat. Mat. **9** 721-724 (2010)

[5] L. Thomas, G. Jan, J. Zhu, H. Liu, Y.-J. Lee, S. Le, R.-Y. Tong, K. Pi, Y.-J. Wang, D. Shen, R. He, J. Haq, J. Teng, V. Lam, K. Huang, T. Zhong, T. Torng, and P.-K.g Wang, "Perpendicular spin transfer torque magnetic random access memories with high spin torque efficiency and thermal stability for embedded applications," JAP **115**, 172615 (2014)

[6] B. S. Tao, D. L. Li, Z. H. Yuan, H. F. Liu, S. S. Ali, J. F. Feng, H. X. Wei, X. F. Han, Y. Liu, Y. G. Zhao, Q. Zhang, Z. B. Guo, and X. X. Zhang," Perpendicular magnetic anisotropy in Ta|Co40Fe40B20|MgAl2O4 structures and perpendicular CoFeB|MgAl2O4|CoFeB magnetic tunnel junction," Appl. Phys. Lett. 105 102407 (2014)

[7] S. Mangin, D. Ravelosona, J. A. Katine, M. J. Carey, B. D. Terris and Eric E Fullerton, "Current-induced magnetization reversal in nanopillars with perpendicular anisotropy," Nature Mat. **5** 210 (2006)

[8] S. Mangin Y. Henry D. Ravelosona , J. A. Katine , and Eric E. Fullerton, "Reducing the critical current for spin-transfer switching of perpendicularly magnetized nanomagnets," Appl. Phys. Lett **94** 012502 ((2009)

[9] A. D. Kent and D. C. Worledge, "A new spin on magnetic memories", Nature Nanotechnology 10, 187 (2015).

[10] D Sander, S O Valenzuela, D Makarov, C H Marrows, E E Fullerton, P Fischer, J McCord, P Vavassori, S Mangin, P Pirro, "The 2017 Magnetism Roadmap", Journal of Physics D: Applied Physics. **50** , 36 (2017)

[11] M. Gottwald, M. Hehn, D. Lacour, T. Hauet, F. Montaigne and S. Mangin, P. Fischer, M.-Y. Im, A. Berger, "Asymmetric magnetization reversal in dipolar-coupled spin valve structures with perpendicular magnetic anisotropy," Phys. Rev. B **85**, 064403 (2012)

[12] Y. Kawato, M. Futamo, and K. Nakamoto, “Perpendicular magnetic recording medium and magnetic storage apparatus,” U.S. Patent US2002/0 028 356 A1, 2002

[13] M. J. Carey, Y. Ikeda, N. Smith, and K. Takano, “Dual-layer perpendicular recording media with laminated underlayer formed with antiferromagnetically coupled films,” U.S. Patent US2003/0 022 023 A1, 2003

[14] A. M. Shukh, E. W. Singleton, S. Khizroev, and D. Litvinov, “Perpendicular recording medium with antiferromagnetic exchange coupling in soft magnetic underlayer,” U.S. Patent US2002/0 028 357 A1, 2002

[15] D. B. Gopman, D. Bedau, S. Mangin, C. H. Lambert, E. E. Fullerton, J. A. Katine, and A. D. Kent, “Asymmetric switching behavior in perpendicularly magnetized spin-valve nanopillars due to the polarizer dipole field,” Appl. Phys. Lett. **100**, 062404 (2012)

[16] L. Cuchet, B.Rodmacq, S.Aufret, R.C. Sousa, I. L. Prejbeanu and B. Dieny, ”Perpendicular magnetic tunnel junctions with a synthetic storage or reference layer: A new route towards Pt- and Pd-free junctions,” Nat. Sci. Rep. **6** 21246 (2016)

[17] D. B. Gopman, D. Bedau, S. Mangin, E. E. Fullerton, J. A. Katine and A. D. Kent, “Switching field distributions with spin transfer torques in perpendicularly magnetized spin-valve nanopillars,” Phys. Rev. B **89**.134427 (2014)

[18] H. Liu, D. Bedau, J. Z. Sun, S. Mangin, E. E. Fullerton, J. A. Katine, and A. D. Kent, “Dynamics of spin torque switching in all-perpendicular spin valve nanopillars,” J.Mag.Mat Mat **358** 233-258 (2014)

[19] R. Skomski, J. Zhou, R.D. Kirby, and D.J. Sellmyer. “Micromagnetic energy barriers,” J. Appl.Phys., **99** 08B906, (2006).

[20] E.M. Lifshitz. L.D. Landau, “Theory of the dispersion of magnetic permeability in ferromagnetic bodies,” Phys. Z. Sowietunion, **8**, 53–169 (1935)

[21] T.L. Gilbert. “A lagrangian formulation of the gyromagnetic equation of the magnetic field,” Phys. Rev. **100**, 1243 (1955)

[22] L. Néel, “Théorie du traînage magnétique des ferromagnétiques en grains fins avec application aux terres 5 cuites,” Ann. Geophys.**5**, 99 (1949)

[23] W.F. Brown, “Thermal fluctuations of a single-domain particle,” Phys. Rev. **130**, 5 (1963)

[24] S. Urazhdin, N.O. Birge, W.P. Pratt Jr., and J. Bass, “Current-driven magnetic excitations in permalloy-based multilayer nanopillars,” Phys. Rev. Lett.**94**, 14 (2003)

[25] Z. Li and S. Zhang, “Magnetization dynamics with a spin-transfer torque,” Phys. Rev. B **68**,024404 (2003)

[26] R.H. Koch, J.A. Katine, and J. Z. Sun, “Time-resolved reversal of spin-transfer switching in a nanomagnet.,” Phys. Rev. Lett. **92**,088302 (2004)

[27] I. Theodonis, N. Kioussis, A. Kalitsov, M. Chshiev, and W.H. Butler, “Anomalous bias dependence of spin torque in magnetic tunnel junctions,” Phys. Rev. Lett. **97**, 237205 (2006)

[28] J.C. Sankey, Y.-T. Cui, J.Z. Sun, J.C. Slonczewski, R.A. Buhrman, and D.C. Ralph, ”Measurement of the spin-transfer-torque vector in magnetic tunnel junctions,” Nat. Phys. **4**, 67–71 (2008)

[29] S. Petit, N. de Mestier, C. Baraduc, C. Thirion, Y. Liu, M. Li, P.Wang, and B. Dieny, “Influence of spin-transfer torque on thermally activated ferromagnetic resonance excitations in magnetic tunnel junctions,” Phys. Rev. B **78**, 184420 (2008)

[30] S. Le Gall, J. Cucchiara, M. Gottwald, C. Berthelot, C.-H. Lambert, Y. Henry, D. Bedau, D. B. Gopman, H. Liu, A. D. Kent, J. Z. Sun, W. Lin, D. Ravelosona, J. A. Katine, Eric E. Fullerton and S. Mangin, “State diagram of nanopillar spin-valve with perpendicular magnetic anisotropy,” Phys. Rev. B **86** 014419 (2012)

[31] Ioan Tudosa, J. A. Katine, S. Mangin, and Eric E. Fullerton, “Phase diagram for spin-torque switching in perpendicular anisotropy magnetic nanopillars,” Appl. Phys. Lett.**96** 212504 (2010)

[32] M Lavanant, S Petit Watelot, AD Kent, S Mangin. “State diagram of a perpendicular magnetic tunnel junction driven by spin transfer torque: a power dissipation approach,” J. Magn Mat Mat **428** 293-299 (2017)

[33] R. Chang, S. Li, M. Lubarda, B. Livshitz, V. Lomakin, “FastMag: Fast micromagnetic simulator for complex magnetic structures,” J. Appl. Phys., **109**,. 07D358 (2011)

[34] K. Bernert, V. Sluka, C. Fowley, J. Lindner, J. Fassbender, and A.M. Deac,”Phase diagrams of mgo magnetic tunnel junctions including the perpendicular spin-transfer torque in different geometries,” Phys. Rev. B, **89**,134415 (2014)

[35] D.C. Worledge, G. Hu, D.W. Abraham, P.L. Trouilloud, and S. Brown. “Development of perpendicularly magnetized Ta|CoFeB|Mgo-based tunnel junctions at IBM,” J. Appl. Phys.,**115** ,172601 (2013)

[36] T. Devolder, A. Le Goff and V. Nikitin “Size dependence of nanosecond-scale spin-torque switching in perpendicularly magnetized tunnel junctions,” Phys. Rev. B, **92**,224432 (2016)